Journal of Medicinal Chemistry

Article

pubs.acs.org/jmc

Positional Scanning Identifies the Molecular Determinants of a High Affinity Multi-Leucine Inhibitor for Furin and PACE4

Izabela Małuch,[#,†] Christine Levesque,[#,‡,§] Anna Kwiatkowska,[*,‡,§] Frédéric Couture,[‡,§] Kévin Ly,[‡,§] Roxane Desjardins,[‡,§] Witold A. Neugebauer,[‡] Adam Prahl,[†] and Robert Day[*,‡,§]

[†]Department of Organic Chemistry, Faculty of Chemistry, University of Gdańsk, 80-308 Gdańsk, Poland

[‡]Institut de Pharmacologie de Sherbrooke, Université de Sherbrooke, 3001 12e Avenue Nord, Sherbrooke J1H 5N4, Canada

[§]Département de Chirurgie/Urologie, Centre Hospitalier Université de Sherbrooke, 3001 12e Avenue Nord, J1H 5N4 Sherbrooke, Canada

S *Supporting Information*

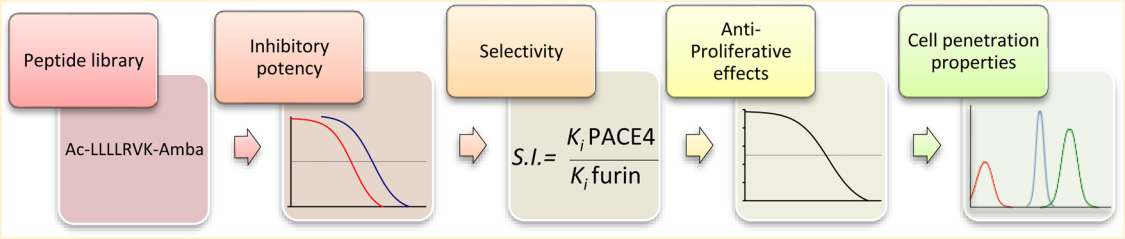

ABSTRACT: The proprotein convertase family of enzymes includes seven endoproteases with significant redundancy in their cleavage activity. We previously described the peptide Ac-LLLLRVK-Amba that displays potent inhibitory effects on both PACE4 and prostate cancer cell lines proliferation. Herein, the molecular determinants for PACE4 and furin inhibition were investigated by positional scanning using peptide libraries that substituted its leucine core with each natural amino acid. We determined that the incorporation of basic amino acids led to analogues with improved inhibitory potency toward both enzymes, whereas negatively charged residues significantly reduced it. All the remaining amino acids were in general well tolerated, with the exemption of the P6 position. However, not all of the potent PACE4 inhibitors displayed antiproliferative activity. The best analogues were obtained by the incorporation of the Ile residue at the P5 and P6 positions. These substitutions led to inhibitors with increased PACE4 selectivity and potent antiproliferative effects.

INTRODUCTION

The family of enzymes known as the proprotein convertases (PCs) includes seven kexin-like members, namely, furin, PC1/3, PC2, PC4, PC5/6, PC7, and PACE4, which process substrates that have the canonical consensus motif R^{P4}-X^{P3}-$(K/R)^{P2}$-R^{P1} (X represents any amino acid).[1−3] The enzymes PC5/6, PC7, and PACE4 are found within constitutive secretory pathways and display a broad tissue distribution pattern, whereas furin is ubiquitously expressed.[1,4−6] The intracellular localization and trafficking of each PC has broad implications with regard to the final effects on precursor processing. Indeed, while distinct *in vivo* functions can be ascribed to individual PCs, significant functional *in vitro* redundancy is also prevalent in this family of enzymes.[7−9] The active site of PCs displays a high level of homology.[3] However, PCs have very different *C*-terminal domains that result in distinct intracellular localization and trafficking and thus confer distinct functions.

PCs have been implicated in the development and progression of various pathologies, including neurodegenerative disorders, osteoarthritis, bacterial and viral infections, and cancer.[1,2,10] For this reason, the exploration of PCs as druggable targets remains an area of significant interest and holds the promise of great potential. To have a pharmacological impact on such complex events, it is essential to better understand the molecular determinants of PCs and their inhibitors.

The determination of the furin crystal structure and the development of PC homology models have aided inhibitor development by providing critical information regarding the composition and disparities between the catalytic clefts.[3,11−14] These studies demonstrated that subsites S1 to S4 are highly similar among all basic amino acid cleaving PCs, with important differences appearing in the S5 and S6 subsites. It was therefore suggested that selective inhibitors would require at least six residues.[3] Recently, our research team developed the first selective PACE4 inhibitor, the octapeptide with the following structure Ac-LLLLRVKR-NH_2.[15] This inhibitor, named the Multi-Leu peptide (compound **1**), displays a 20-fold selectivity, with K_is of 22 ± 6 nM for PACE4 and 430 ± 10 nM for furin.[15] This study confirmed that the S5−S6 subsites, as well as the S7 subsite (and to a certain extent the S8 subsite), could be utilized to develop inhibitors that distinguish between various

Received: October 14, 2016
Published: March 13, 2017

DOI: 10.1021/acs.jmedchem.6b01499
J. Med. Chem. 2017, 60, 2732−2744

PCs. Most notably, PACE4 is well inhibited by a peptide with hydrophobic amino acids in these positions, while furin is not.

With regard to the potential clinical usefulness of such inhibitors, the peptide **1** exhibits antiproliferative effects on the DU145 and LNCaP prostate cancer cell lines. Both cell lines express high levels of PACE4, while another prostate cancer cell line, PC3, does not express PACE4. PC3 cell proliferation is not affected by peptide **1**. There are additional lines of evidence demonstrating the important role of PACE4 in the progression of prostate cancer.[16,17] PACE4 is the only PC that is upregulated in malignant samples of prostate tissues, which was shown at both the mRNA[16,18,19] and protein levels.[18,19] PACE4 also displays a unique role in cancer progression *in vivo*,[17] supporting the hypothesis that PACE4 inhibitors may be an important tool for prostate cancer therapy. With this therapeutic indication in mind, it might be strategically important to develop stable and high affinity PACE4 inhibitors with limited potency toward the other PCs. These can be based on the backbone of peptide **1**, with modifications using peptidomimetic strategies, which should result in compounds that will be optimal for *in vivo* use.

To achieve this objective, structure–activity relationship studies were performed to evaluate potential modifications.[20] Recent work has focused on the substitution of the Arg^{P1} residue of furin inhibitors with the unnatural arginine mimetic 4-amidinobenzylamide (Amba), resulting in important gains in inhibitory potency,[21−23] and demonstrating the favorable conformation of this mimetic for tight binding of the PC active site.[14] We have carried out similar work with our peptide **1** inhibitor, synthesizing an Amba-substituted version of this peptide (Ac-LLLLRVK-Amba, peptide **2**). We confirmed an important increase (7-fold) in inhibitory potency against PACE4 (K_i PACE4:3.1 ± 0.8 nM).[20] However, the introduction of the Amba moiety into inhibitor **1** also increased the inhibitory potency toward furin, which is likely due to the high affinity of the Amba residue for furin subsite S1 (K_i furin: 4.3 ± 0.8 nM).

While the significant increase in potency is desirable, the lack of selectivity may be problematic in regard to a therapeutic application of the inhibitor. Therefore, we undertook a structure–activity study using peptide **2** as a scaffold in order to explore potential molecular determinants that could be substituted, while preserving potency and improving selectivity. We designed a positional scan library substituting the P5–P8 positions, while maintaining the important PC recognition motif in the P1–P4 positions. The library consists of 73 pure peptides (a reference analogue (**2**) and 18 peptides for each scan position; the P5 library, analogues **3–20**; the P6 library, analogues **21–38**; the P7 library, analogues **39–56**, the P8 library: analogues **57–74**; Figure 1). Although our primary indicator is the inhibition constant (K_i value), we also tested these peptides in cell-based assays using LNCaP and DU145 cell lines. Based on these results, we decided further to evaluate the cell penetrating properties of the selected inhibitors.

Library		P8	P7	P6	P5	P4	P3	P2	P1
P5	Ac-	L	L	L	X	R	V	K	Amba
P6	Ac-	L	L	X	L	R	V	K	Amba
P7	Ac-	L	X	L	L	R	V	K	Amba
P8	Ac-	X	L	L	L	R	V	K	Amba

Figure 1. Positional scanning in the leucine extension of the lead compound Ac-LLLLRVK-Amba (peptide **2**). Letter X designates every naturally occurring amino acid, with the exception of cysteine.

RESULTS

Peptide Synthesis. The first series of inhibitors (P5-substituted peptides) was synthesized using 4-Fmoc-hydrazinobenzoyl resin (Scheme 1). Briefly, the P8–P2 segments were simultaneously assembled on the resin using standard Fmoc solid-phase peptide synthesis (SPPS). The removal of the protected peptide from the resin was achieved in two steps, including oxidation of the hydrazine moiety to diazene with copper(II) acetate followed by the coupling of the protected Amba. The final compound was obtained after the side-chain deprotection with trifluoroacetic acid (TFA) and the liberation of the amidine group by hydrogenation. Although this synthetic route afforded the desired compounds, the laborious operations, difficulties in monitoring peptide cleavage from the resin and low yields of the entire synthesis process (not higher than 20% after attempts to optimize the oxidation process) motivated us to find another, more efficient synthetic route. The remaining inhibitors were prepared by a combination of SPPS and solution-phase synthesis using 2-chlorotrityl-chloride resin as previously described (Scheme 2).[20] In brief, the Fmoc-Lys(Boc)-OH was manually attached to the resin in the presence of *N*,*N*-diisopropylethylamine (DIPEA) and then standard protocols for SPPS were employed to synthesize the P8–P2 segment. The protected peptide was cleaved under mild acidic conditions followed by the coupling

Scheme 1. Synthesis of the P5 Inhibitor Library[a]

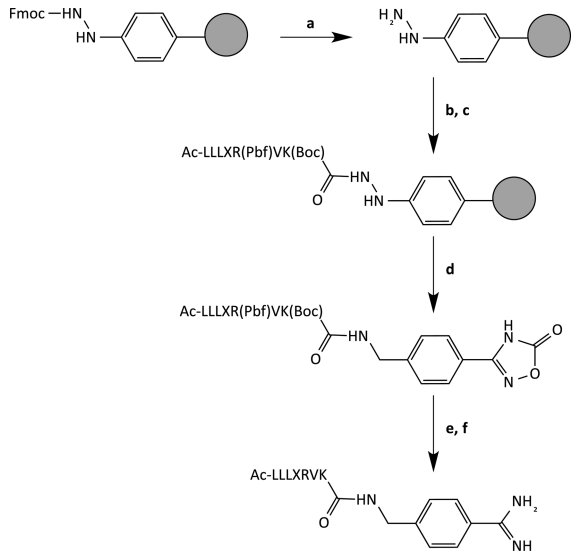

[a]With the exception of compound **11**, the peptides of the Ac-LLLXRVK-Amba library were synthesized using the following steps: (a) removal of protecting group from 4-Fmoc-hydrazinobenzoyl resin, 20% piperidine/DMF; (b) Fmoc SPPS, triple coupling with 2.5 equiv of amino acid, TBTU and HOBt, 5 equiv of NMM; (c) triple coupling of the acetyl group, acetic anhydride/DIPEA/DCM (1.5/1.5/7, v/v/v), 10 min; (d) oxidation of the peptidyl resin and coupling 3-[4-(aminomethyl)phenyl]-1,2,4-oxadiazol-5(4*H*)-one, 2.5 equiv of the protected 4-amidinobenzylamine, 0.7 equiv of $Cu(OAc)_2$, 1.5 equiv of pyridine in anhydrous DMF, 24 h; (e) TFA/TIS/H_2O (95/2.5/2.5, v/v/v), 2.5 h; and (f) hydrogenation in acetic acid/MeOH (1:1, v/v) with 10% Pd/C as a catalyst, 55 psi, 1.5 h.

DOI: 10.1021/acs.jmedchem.6b01499
J. Med. Chem. 2017, 60, 2732−2744

Scheme 2. Analogue Synthesis Using 2-Chlorotrityl-chloride Resin (on the Example of the P6 Inhibitor Library)[a]

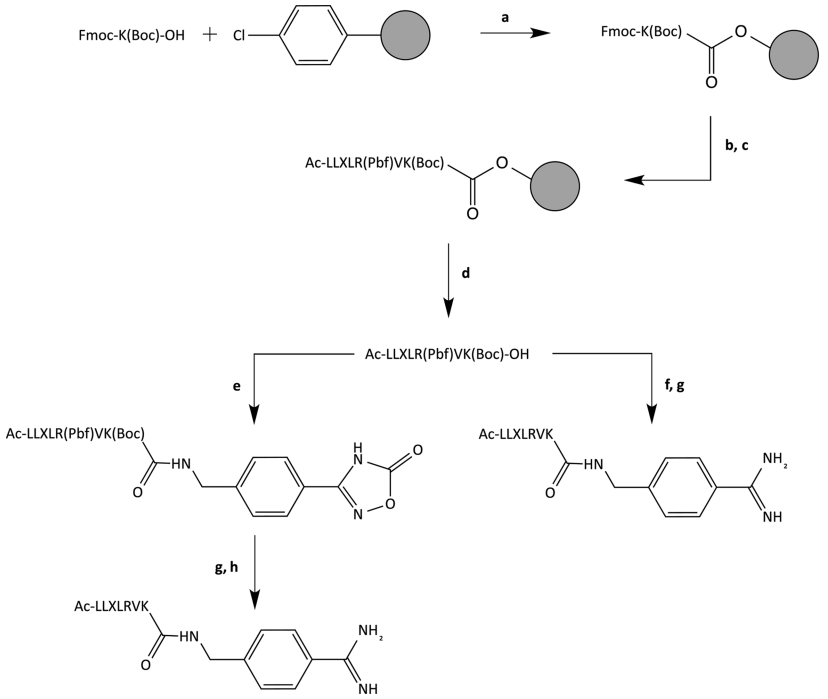

[a]Analogue synthesis using 2-chlorotrityl-chloride resin was performed using the following steps: (a) loading of 2-chlorotrityl-chloride resin, 2 equiv of Fmoc-Lys(Boc)-OH, 2 equiv of DIPEA, dry DCM, 1.5 h; (b) Fmoc SPPS (for conditions, see Scheme 1); (c) triple coupling of the acetyl group (for conditions, see Scheme 1); (d) cleavage from the resin, HFIP/TFE/DCM (3/2/5, v/v/v); (e) 3-[4-(aminomethyl)phenyl]-1,2,4-oxadiazol-5(4*H*)-one coupling, 2 equiv of the protected 4-amidinobenzylamine, 2 equiv of COMU, 8 equiv of NMM in anhydrous DMF, 12 h; (f) 3 equiv of 4-amidinobenzylamine ·2HCl Amba, 3 equiv of COMU, 8 equiv of NMM or 6 equiv of DIPEA in anhydrous DMF, 12 h; (g) TFA/TIS/H_2O (95/2.5/2.5, v/v/v), 2.5 h; and (h) hydrogenation (for conditions, see Scheme 1).

of protected 4-amidinobenzylamine or 4-amidinobenzylamine·2HCl, and then final removal of all protecting groups. This synthetic route proved to be robust, simple, and reliable.

Fluorescent versions of the selected inhibitors were also obtained using this synthetic route. In these cases, the P8−P2 segment was *N*-terminally modified with isothiocyanate isomer I (FITC) group via *β*Ala residue, which was used as a spacer. All peptides were analyzed by liquid chromatography mass spectrometry with electrospray ionization (LCMS ESI IT-TOF) or high-resolution mass spectrometry (HRMS) and reversed-phase high-performance liquid chromatography (RP-HPLC). The purification was performed using RP-HPLC, and all analogues were obtained as lyophilized trifluoroacetic (TFA) salts. The analytical data of all analogues are presented as Supporting Information in Table S1.

Enzymatic Studies. To identify the molecular determinants for PC inhibition, a positional scanning library was designed from the initial scaffold **2** (Figure 1). The library was screened against PACE4 and furin, and the K_is were determined to compare the binding affinities of each peptide in the library. All of the tested peptides showed an inhibitory effect at very low concentrations comparable with the concentration of the enzyme used; therefore, their K_is were calculated using the Morrison equation for reversible tight-binding inhibition.[24,25] As described previously, K_is for peptide **2** are in the low nanomolar range for both enzymes, with values of 3.1 ± 0.8 and 4.3 ± 0.8 nM for PACE4 and furin, respectively.[20]

Position P5. The library screen comparing residues in the P5 position revealed a strong influence of charge composition at this position (Figure 2A). Indeed, a major difference in PACE4 binding properties was observed for peptides containing positively charged residues as analogue **15** (K_i: 0.2 ± 0.1 nM), analogue **10** (K_i: 2 ± 1 nM), and analogue **8** (K_i: 0.4 ± 0.3 nM) versus negatively charged residues as peptide **4** (K_i: 400 ± 90 nM) and peptide **5** (K_i: 46 ± 9 nM), with a nearly 2000-fold increase in K_i values between peptide **10** and analogue **4**. The same trend was observed for furin, with K_i values between 0.7 ± 0.4 nM (analogue **15**) and 230 ± 60 nM (analogue **4**). The high impact of charges within this position was also previously described by Becker et al.,[22] whereas the addition of basic moieties in position P5 increased the overall affinity of Amba-containing peptides for furin.

With the exception of negatively charged amino acids, PACE4 tolerated a broad range of amino acid substitutions at the P5 position, and uncharged residues presented K_is in the 10^{-9} M range. However, the Gly substituted peptide (analogue **7**) seemed unfavorable for both PACE4 and furin, with K_i values of 18 ± 6 and 12 ± 4 nM, respectively. Because the Gly residue differs from other amino acid by its greater conformational flexibility, these low values could indicate that the additional freedom in the peptide chain destabilizes the molecular interactions between the peptide and active site cleft. Furthermore, analogue **9** with an Ile residue seems to be unfavorable for furin (K_i: 29 ± 9 nM) and tolerated by PACE4 (K_i: 8 ± 3 nM).

To identify possible substitutions that could result in a selective and potent inhibitor, a selectivity index was calculated from the ratio between the furin and PACE4 inhibition constants for each peptide (Figure 3A). As seen from these

DOI: 10.1021/acs.jmedchem.6b01499
J. Med. Chem. 2017, 60, 2732−2744

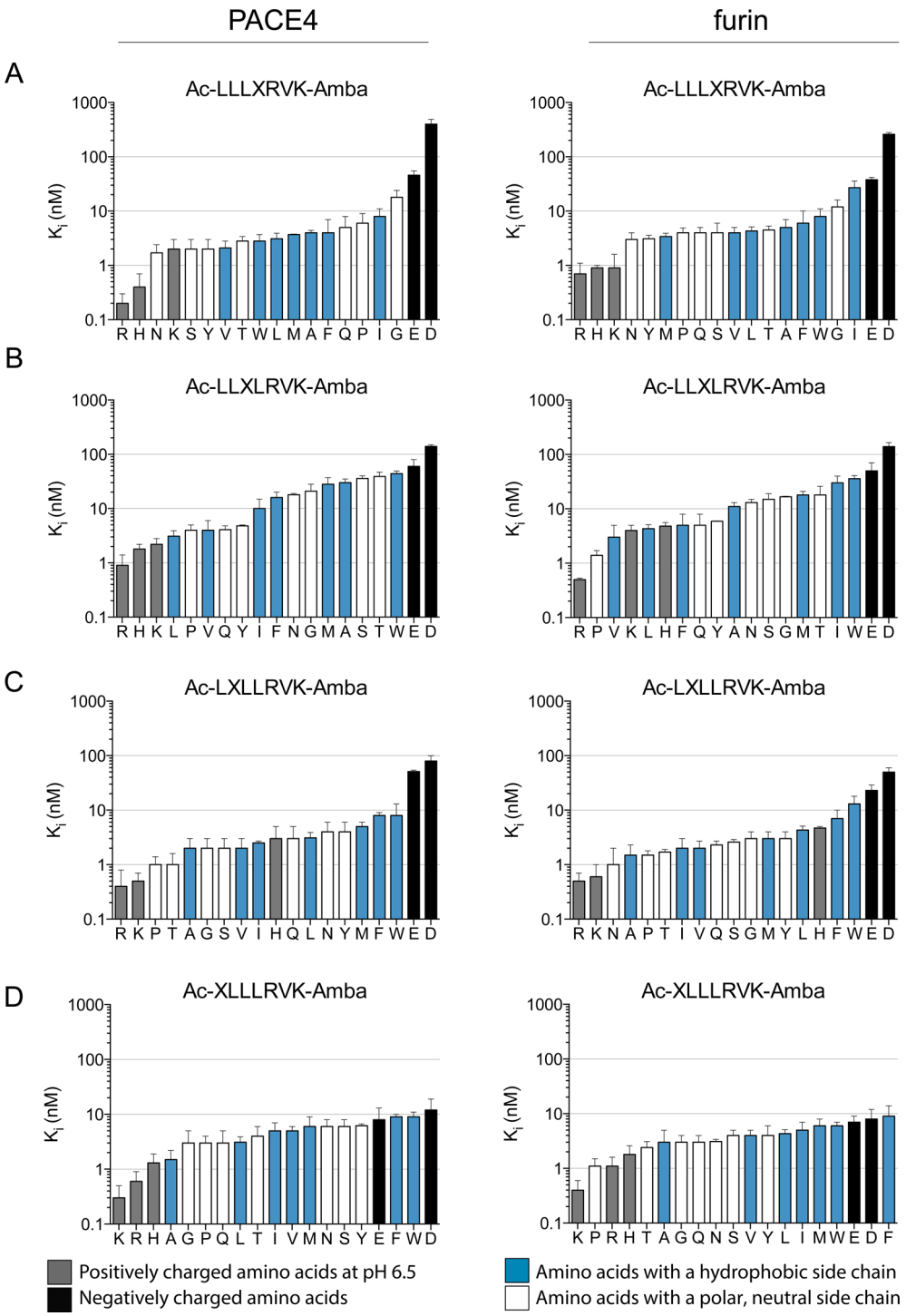

Figure 2. Screening the P5 to P8 libraries with recombinant PACE4 and furin. K_is were obtained by screening the libraries against PACE4 and furin and were classified according to the observed affinity. Amino acids colored according to the classification by Eisenberg.[26]

selectivity indexes, a few residues offered an increase in selectivity when compared to Leu in the P5 position. Five residues displayed at least a 2-fold selectivity for PACE4 over furin, namely, His (2.3-fold), Ile (3.4-fold), Arg (3.5-fold), Ser (2.0-fold), and Trp (2.9-fold).

Position P6. The evaluation of K_i values for the P6 peptide library demonstrated an attenuated importance of positively charged amino acid residues for PACE4 in this position (Figure 2B). Indeed, the inhibitory potency of analogue **33** (K_i: 0.9 ± 0.5 nM), peptide **28** (K_i: 2.2 ± 0.6 nM), and compound **26** (K_i: 1.8 ± 0.4 nM) was less important in the P6 position than for any other position since **33** reached nearly subnanomolar inhibition, whereas **28** and **26** offered only nanomolar inhibition. The same trend was observed for furin, where only inhibitor **33** (K_i: 0.50 ± 0.03 nM) demonstrated subnanomolar inhibition. Furthermore, the K_is obtained for the P6 library demonstrated an overall elevated inhibitory profile compared to the P5 library. Whereas most peptides displayed K_is below 10 nM toward PACE4 in position P5, only eight peptides from the P6 library displayed binding properties

DOI: 10.1021/acs.jmedchem.6b01499
J. Med. Chem. 2017, 60, 2732−2744

A. Position P5

		K_i PACE4 (nM)	K_i furin (nM)	Selectivity index
2	Ac- L L L L R V K - Amba	3.1 ± 0.8	4.3 ± 0.8	1.4
3	Ac- L L L A R V K - Amba	4.0 ± 0.4	5 ± 2	1.3
4	Ac- L L L D R V K - Amba	400 ± 90	260 ± 20	0.6
5	Ac- L L L E R V K - Amba	46 ± 9	38 ± 4	0.8
6	Ac- L L L F R V K - Amba	4 ± 3	6 ± 4	1.5
7	Ac- L L L G R V K - Amba	18 ± 6	12 ± 4	0.7
8	Ac- L L L H R V K - Amba	0.4 ± 0.3	0.9 ± 0.1	2.3
9	Ac- L L L I R V K - Amba	8 ± 3	27 ± 9	3.4
10	Ac- L L L K R V K - Amba	2 ± 1	0.9 ± 0.7	0.5
11	Ac- L L L M R V K - Amba	3.7 ± 0.1	3.4 ± 0.5	0.9
12	Ac- L L L N R V K - Amba	1.7 ± 0.7	3 ± 1	1.8
13	Ac- L L L P R V K - Amba	6 ± 3	4.0 ± 0.9	0.7
14	Ac- L L L Q R V K - Amba	5 ± 3	4 ± 1	0.8
15	Ac- L L L R R V K - Amba	0.2 ± 0.1	0.7 ± 0.4	3.5
16	Ac- L L L S R V K - Amba	2 ± 1	4 ± 2	2.0
17	Ac- L L L T R V K - Amba	2.8 ± 0.6	4.5 ± 0.8	1.6
18	Ac- L L L V R V K - Amba	2.1 ± 0.7	4 ± 1	1.9
19	Ac- L L L W R V K - Amba	2.8 ± 0.9	8 ± 3	2.9
20	Ac- L L L Y R V K - Amba	2 ± 1	3.1 ± 0.5	1.6

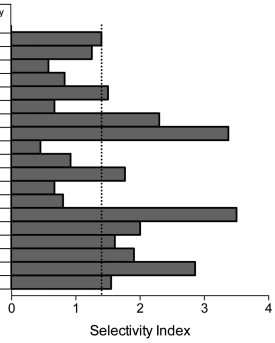

B. Position P6

		K_i PACE4 (nM)	K_i furin (nM)	Selectivity index
2	Ac- L L L L R V K - Amba	3.1 ± 0.8	4.3 ± 0.8	1.4
21	Ac- L L A L R V K - Amba	30 ± 5	11 ± 2	0.4
22	Ac- L L D L R V K - Amba	140 ± 10	140 ± 30	1.0
23	Ac- L L E L R V K - Amba	60 ± 20	50 ± 20	0.8
24	Ac- L L F L R V K - Amba	16 ± 4	5 ± 3	0.3
25	Ac- L L G L R V K - Amba	21 ± 7	16.7 ± 0.3	0.8
26	Ac- L L H L R V K - Amba	1.8 ± 0.4	4.8 ± 0.8	2.7
27	Ac- L L I L R V K - Amba	10 ± 5	30 ± 10	3.0
28	Ac- L L K L R V K - Amba	2.2 ± 0.6	4 ± 1	1.8
29	Ac- L L M L R V K - Amba	28 ± 9	18 ± 3	0.6
30	Ac- L L N L R V K - Amba	18 ± 1	13 ± 2	0.7
31	Ac- L L P L R V K - Amba	4 ± 1	1.4 ± 0.3	0.4
32	Ac- L L Q L R V K - Amba	4.1 ± 0.7	5 ± 3	1.2
33	Ac- L L R L R V K - Amba	0.9 ± 0.5	0.50 ± 0.03	0.6
34	Ac- L L S L R V K - Amba	36 ± 4	15 ± 4	0.4
35	Ac- L L T L R V K - Amba	39 ± 8	18 ± 8	0.5
36	Ac- L L V L R V K - Amba	4 ± 2	3 ± 2	0.8
37	Ac- L L W L R V K - Amba	44 ± 5	36 ± 5	0.8
38	Ac- L L Y L R V K - Amba	4.8 ± 0.2	5.9 ± 0.1	1.2

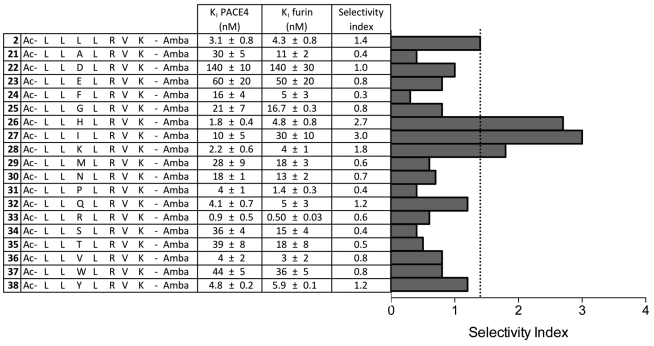

C. Position P7

		K_i PACE4 (nM)	K_i furin (nM)	Selectivity index
2	Ac- L L L L R V K - Amba	3.1 ± 0.8	4.3 ± 0.8	1.4
39	Ac- L A L L R V K - Amba	2 ± 1	1.5 ± 0.8	0.8
40	Ac- L D L L R V K - Amba	80 ± 20	50 ± 10	0.6
41	Ac- L E L L R V K - Amba	51 ± 3	23 ± 6	0.5
42	Ac- L F L L R V K - Amba	8 ± 1	7 ± 3	0.9
43	Ac- L G L L R V K - Amba	2 ± 1	3 ± 1	1.5
44	Ac- L H L L R V K - Amba	3 ± 2	4.7 ± 0.3	1.6
45	Ac- L I L L R V K - Amba	2.5 ± 0.2	2 ± 1	0.8
46	Ac- L K L L R V K - Amba	0.5 ± 0.2	0.6 ± 0.4	1.2
47	Ac- L M L L R V K - Amba	5 ± 1	3 ± 1	0.6
48	Ac- L N L L R V K - Amba	4 ± 2	1 ± 1	0.3
49	Ac- L P L L R V K - Amba	1.0 ± 0.4	1.5 ± 0.3	1.5
50	Ac- L Q L L R V K - Amba	3 ± 2	2.3 ± 0.4	0.8
51	Ac- L R L L R V K - Amba	0.4 ± 0.4	0.5 ± 0.2	1.3
52	Ac- L S L L R V K - Amba	2 ± 1	2.6 ± 0.3	1.3
53	Ac- L T L L R V K - Amba	1.0 ± 0.6	1.7 ± 0.2	1.7
54	Ac- L V L L R V K - Amba	2 ± 1	2.0 ± 0.7	1.0
55	Ac- L W L L R V K - Amba	8 ± 5	13 ± 5	1.6
56	Ac- L Y L L R V K - Amba	4 ± 2	3 ± 1	0.8

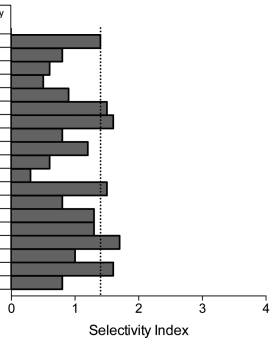

D. Position P8

		K_i PACE4 (nM)	K_i furin (nM)	Selectivity index
2	Ac- L L L L R V K - Amba	3.1 ± 0.8	4.3 ± 0.8	1.4
57	Ac- A L L L R V K - Amba	1.5 ± 0.7	3 ± 2	2.0
58	Ac- D L L L R V K - Amba	12 ± 7	8 ± 4	0.7
59	Ac- E L L L R V K - Amba	8 ± 5	7 ± 2	0.9
60	Ac- F L L L R V K - Amba	9 ± 1	9 ± 5	1.0
61	Ac- G L L L R V K - Amba	3 ± 2	3 ± 1	1.0
62	Ac- H L L L R V K - Amba	1.3 ± 0.6	1.8 ± 0.8	1.4
63	Ac- I L L L R V K - Amba	5 ± 2	5 ± 2	1.0
64	Ac- K L L L R V K - Amba	0.3 ± 0.2	0.4 ± 0.2	1.3
65	Ac- M L L L R V K - Amba	6 ± 3	6 ± 2	1.0
66	Ac- N L L L R V K - Amba	6 ± 2	3.1 ± 0.3	0.5
67	Ac- P L L L R V K - Amba	3 ± 1	1.1 ± 0.4	0.4
68	Ac- Q L L L R V K - Amba	3 ± 2	3 ± 1	1.0
69	Ac- R L L L R V K - Amba	0.6 ± 0.3	1.1 ± 0.5	1.8
70	Ac- S L L L R V K - Amba	6 ± 2	4 ± 1	0.7
71	Ac- T L L L R V K - Amba	4 ± 2	2.4 ± 0.7	0.6
72	Ac- V L L L R V K - Amba	5 ± 1	4 ± 1	0.8
73	Ac- W L L L R V K - Amba	9 ± 2	6 ± 1	0.7
74	Ac- Y L L L R V K - Amba	6.2 ± 0.5	4 ± 2	0.6

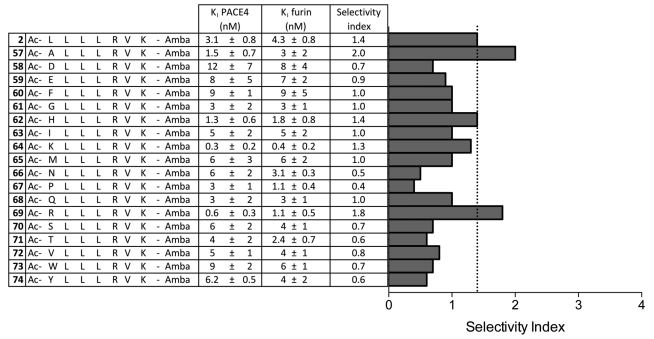

Figure 3. Selectivity index toward PACE4. The selectivity index (K_i Furin/K_i PACE4) was calculated from the inhibition constants to indicate the discrimination between PACE4 and furin for each substitution. The data in the table are the mean values ± SD of three independent experiments.

in the 10^{-9} M range, including inhibitors modified with basic residues (analogues **26**, **28**, and **33**), Pro (peptide **31**, K_i: 4 ± 1 nM), Val (peptide **36**, K_i: 4 ± 2 nM), Gln (peptide **32**, K_i: 4.1 ± 0.7 nM), Tyr (peptide **38**, K_i: 4.8 ± 0.2 nM), and Leu in the initial scaffold **2** (K_i: 3.1 ± 0.8 nM). Interestingly, we previously reported results from a partial combinatorial library, where the presence of Leu in position P6 resulted in a strong affinity for PACE4, with a K_i value in the same range as peptides with Lys and Arg at this position.[15] This result suggests that Leu residue in the P6 position greatly contributes to inhibitory properties of peptide **1** toward PACE4.

The selectivity indexes were calculated for the P6 library screen against PACE4 and furin and indicated that only two peptides offered a selectivity of at least 2-fold toward PACE4. Peptides containing Ile (analogue **27**) and His (analogue **26**) displayed selectivity indices of 3.0 and 2.7, respectively (Figure 3).

Position P7. In the Ac-LXLLRVK-Amba library, all peptides with exception of the negatively charged analogue **40** (K_i: 80 ± 20 nM) and analogue **41** (K_i: 51 ± 3 nM) displayed K_is below 10 nM for PACE4 (Figure 2C). Although His containing peptides were among the best PACE4 inhibitors at the other positions, compound **44** (K_i: 3 ± 2 nM) displayed average inhibition at the P7 site, whereas other basic residues led to analogues **51** (K_i: 0.4 ± 0.4 nM) and **46** (K_i: 0.5 ± 0.2 nM) with subnanomolar inhibition. The same trend was observed for furin, with a K_i of 4.7 ± 0.3 nM for peptide **44** versus subnanomolar inhibition by analogue **51** (K_i: 0.5 ± 0.2 nM) and analogue **46** (K_i: 0.6 ± 0.4 nM). Furthermore, large amino acids containing aromatic moieties such as Trp (peptide **55**, K_i PACE4:8 ± 5 nM; furin: 13 ± 5 nM) and Phe (peptide **42**, K_i PACE4:8 ± 1 nM; furin: 7 ± 3 nM) showed slight disadvantages compared to other residues. Therefore, flexibility constraints or steric hindrance due to side chain composition could explain the disadvantage of the residues Trp, Phe, and His for both PACE4 and furin (Figure 2). However, inhibition for those peptides remained in the low nanomolar range.

The P7 library screen revealed very similar inhibitory profiles for PACE4 and furin. Indeed, only slight differences were observed between the selectivity indexes calculated for every substitution (Figure 3). This suggests that, although position P7 appears to participate in peptide affinity, subsite S7 could not be exploited for molecular discrimination of both enzymes into a high affinity PACE4 inhibitor.

Position P8. The analysis of residues' contribution to the P8 position in the Ac-XLLLRVK-Amba library demonstrated an attenuated influence of amino acid substitutions at this position (Figure 2D). Indeed, although the basic residues Lys (analogue **64**, K_i: 0.3 ± 0.2 nM), Arg (peptide **69**, K_i: 0.6 ± 0.3 nM), and His (analogue **62**, K_i: 1.3 ± 0.6 nM) offered potent inhibition toward PACE4, the K_i values obtained for other residues were in a narrow range, from 1.5 nM for Ala (analogue **57**) to 12 nM for Asp (analogue **58**). Furthermore, negative residues presented in peptides **59** (K_i: 8 ± 5 nM) and **58** (K_i: 12 ± 7 nM), did not offer a substantial inhibitory disadvantage, as opposed to the results obtained for positions P5, P6, and P7. Thus, whereas basic residues contributed to inhibition at this position, the P8 library screen demonstrated a minimal impact of residue substitutions on the initial scaffold (**2**), suggesting that the P8 residue of the inhibitors would be outside the binding cleft of PCs.

Consistent with this observation, no residue seems to offer discrimination between PACE4 and furin as observed from the

DOI: 10.1021/acs.jmedchem.6b01499
J. Med. Chem. 2017, 60, 2732−2744

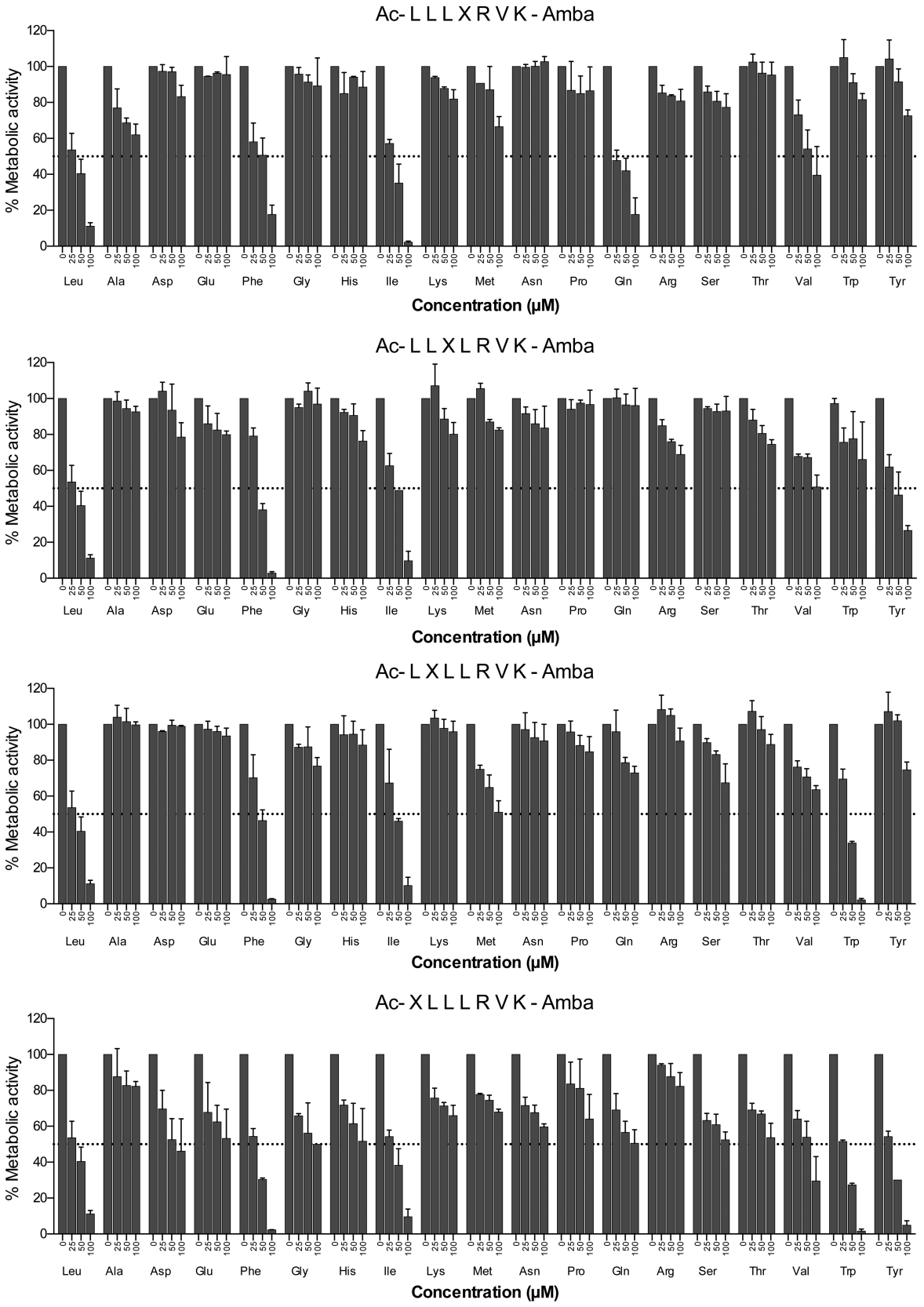

Figure 4. Inhibitory potency of peptides on DU145 cell proliferation. The proliferation assay was performed for every peptide of the library using DU145 cells at doses of 0, 25, 50, and 100 μM in an MTT assay. The data in the histogram are the mean values ± SEM of at least two independent experiments.

selectivity index. With the exception of peptide **57** (2.0-fold selectivity) all of the selectivity indexes were below 2.0.

Proliferation Studies. As described previously, the ML peptide and its analogues display antiproliferative effects on

DOI: 10.1021/acs.jmedchem.6b01499
J. Med. Chem. 2017, 60, 2732−2744

DU145 and LNCaP prostate cancer cell lines, which both express the enzyme PACE4 at significant levels.[15,17] To evaluate the antiproliferative effects of each peptide in the P5 to P8 libraries, proliferation studies were performed at doses of 25, 50, and 100 μM on DU145 cells (Figure 4). Peptides with antiproliferative effects on DU145 cells were selected for further proliferation assays using peptide doses of 1, 10, 25, 50, 75, and 100 μM on DU145 and LNCaP cell lines, and the IC_{50} values were calculated from the inhibition curves (Table 1). In

Table 1. IC_{50}s Calculated from the Dose−Response Curves Using DU145 and LNCaP Cell Lines[a]

		DU145	LNCaP
		IC_{50} (μM)	IC_{50} (μM)
1	Ac- **L L L L** R V K R - NH_2	100 ± 10	180 ± 60
2	Ac- **L L L L** R V K -Amba	25 ± 10	40 ± 15
6	Ac- L L L **F** R V K - Amba	40 ± 10	50 ± 20
9	Ac- L L L **I** R V K - Amba	50 ± 10	28 ± 6
14	Ac- L L L **Q** R V K - Amba	12 ± 1	26 ± 9
18	Ac- L L L **V** R V K - Amba	45 ± 7	60 ± 10
24	Ac- L L **F** L R V K - Amba	38 ± 2	40 ± 10
27	Ac- L L **I** L R V K - Amba	32 ± 4	80 ± 10
38	Ac- L L **Y** L R V K - Amba	50 ± 10	130 ± 40
42	Ac- L **F** L L R V K - Amba	36 ± 7	31 ± 9
45	Ac- L **I** L L R V K - Amba	31 ± 5	40 ± 8
55	Ac- L **W** L L R V K - Amba	35 ± 6	50 ± 20
58	Ac- **D** L L L R V K - Amba	90 ± 4	40 ± 10
59	Ac- **E** L L L R V K - Amba	150 ± 20	120 ± 30
60	Ac- **F** L L L R V K - Amba	30 ± 10	41 ± 5
63	Ac- **I** L L L R V K - Amba	27 ± 5	40 ± 10
68	Ac- **Q** L L L R V K - Amba	150 ± 40	>250
70	Ac- **S** L L L R V K - Amba	100 ± 22	>250
71	Ac- **T** L L L R V K - Amba	140 ± 10	110 ± 20
72	Ac- **V** L L L R V K - Amba	75 ± 20	70 ± 20
73	Ac- **W** L L L R V K - Amba	23 ± 4	39 ± 3
74	Ac- **Y** L L L R V K - Amba	23 ± 6	160 ± 20

[a]Peptides with antiproliferative effects on DU145 cells were selected for further analysis with the DU145 and LNCaP prostate cancer cell lines. IC_{50} values were calculated from the dose−response curves obtained from the MTT assay. The data in the table are the means ± SEM of three independent experiments.

position P5, IC_{50}s were calculated from selected peptides containing analogue **6** (DU145, 40 ± 10 μM; LNCaP, 50 ± 20 μM), analogue **9** (DU145, 50 ± 10 μM; LNCaP, 28 ± 6 μM), analogue **14** (DU145, 12 ± 1 μM; LNCaP, 26 ± 9 μM), and analogue **18** (DU145, 45 ± 7 μM; LNCaP, 60 ± 10 μM). While analogues **6**, **9**, and **18** exhibited similar antiproliferative effects on both DU145 and LNCaP cells, peptide **14** presented a 2-fold improvement when compared to the control peptide **2**. In the position P6, only analogues containing Phe (analogue **24**), Ile (analogue **27**), or Tyr (analogue **38**) exhibited inhibitory effects on DU145 cell proliferation (Figure 4). Calculation of IC_{50}s demonstrated that peptides with Phe (**24**, DU145, 38 ± 2 μM; LNCaP, 40 ± 10 μM) or Ile (**27**, DU145, 32 ± 4 μM; LNCaP, 80 ± 10 μM) were equally potent relative to the control peptide **2**, whereas substitution with Tyr (**38**, DU145, 50 ± 10 μM; LNCaP, 130 ± 40 μM) altered the inhibitory effects on both DU145 and LNCaP cells (Table 1). Screening for position P7 revealed that only three peptides were capable of inhibiting DU145 cell proliferation (Figure 4), and determination of the IC_{50}s for these peptides containing Phe (analogue **42**, DU145, 36 ± 7 μM; LNCaP, 40 ± 10 μM), Ile (analogue **45**, DU145, 31 ± 5 μM; LNCaP, 40 ± 8 μM), or Trp (analogue **55**, DU145, 50 ± 10 μM; LNCaP, 130 ± 40 μM) substitutions demonstrated that all of the peptides displayed similar inhibitory properties as the initial scaffold **2**. In the P8 position (Figure 4), several peptides displayed antiproliferative effects on DU145 and LNCaP cells. Whereas peptides containing Phe (analogue **60**, DU145, 30 ± 10 μM; LNCaP, 41 ± 5 μM), Ile (analogue **63**, DU145, 27 ± 5 μM; LNCaP, 40 ± 10 μM), and Trp (analogue **73**, DU145, 23 ± 4 μM; LNCaP, 39 ± 3 μM) displayed similar inhibition properties to the control peptide **2** on both DU145 and LNCaP cells, substitution with Asp (analogue **58**, DU145, 90 ± 4 μM; LNCaP, 40 ± 10 μM), Glu (analogue **59**, DU145, 150 ± 20 μM; LNCaP, 120 ± 30 μM), Gln (analogue **68**, DU145, 150 ± 40 μM LNCaP, >250 μM), Ser (analogue **70**, DU145:100 ± 22 μM; LNCaP, >250 μM), Thr (analogue **71**, DU145, 140 ± 10 μM; LNCaP, 110 ± 20 μM), Val (analogue **72**, DU145, 75 ± 20 μM; LNCaP, 70 ± 20 μM), and Tyr (analogue **74**, DU145, 23 ± 6 μM; LNCaP, 160 ± 20 μM) decreased inhibitory potency in the cell-based assay.

Of all the analogues tested in this experiment, only compound **14** showed increased antiproliferative effects compared with the previously described control peptide **2**.[20] For every position tested, peptides substituted with Phe or Ile displayed similar antiproliferative properties when compared to the lead compound. Interestingly, according to Eisenberg's hydrophobicity classification of amino acids, these two residues are the most hydrophobic residues among the 20 natural amino acids.[26] Furthermore, peptides substituted with Val at the P5 position (analogue **18**), Trp at the P7 position (analogue **55**), and Trp at the P8 position (analogue **73**) also offered potent antiproliferative effects on both DU145 and LNCaP cells and feature hydrophobic side chains. With the exception of the polar Gln residue at the P5 position (analogue **14**), every peptide that displayed inhibition in the low micromolar range on both prostate cancer cell lines was substituted with highly hydrophobic residues. This observation suggests that the hydrophobic nature of the P5−P8 core of scaffold **2** is a critical feature to preserve antiproliferative effects, and this information should be taken into account for further optimization of PACE4 inhibitors.

Cell Penetration. Since our previous studies demonstrated the need for cell permeability of PACE4 inhibitors in order to elicit antiproliferative effects, we ought to assess ability of our new compounds to penetrate cells. We therefore selected two analogues based on their *in vitro* inhibitory activity, **9** and **15**, and determined their cellular uptake. Both inhibitors display potent activity against recombinant PACE4; however, only analogue **9** exhibits antiproliferative effect on prostate cancer cell lines. To compare the quantity of the internalized peptides, the FITC-labeled derivatives of both analogues were prepared and analyzed by flow cytometry after 1 h incubation with DU145 cells. False-positive signals resulting from nonspecific interactions with membrane proteins were eliminated after extensive trypsinization. Quantitative assessment of cell penetration of each peptide in comparison with the initial scaffold (FITC-βAla-LLLLRVK-Amba, compound **75**)[27] is presented in Figure 5. The fluorescent version of peptide **15** (FITC-βAla-LLLRRVK-Amba, compound **76**) showed the lowest cellular uptake with the geometric mean fluorescence intensity (GMFI) of 12.60 and 2.73 without and with trypsin wash, respectively. However, the fluorescent derivative of inhibitor **9** (FITC-βAla-LLLIRVK-Amba, compound **77**)

DOI: 10.1021/acs.jmedchem.6b01499
J. Med. Chem. 2017, 60, 2732−2744

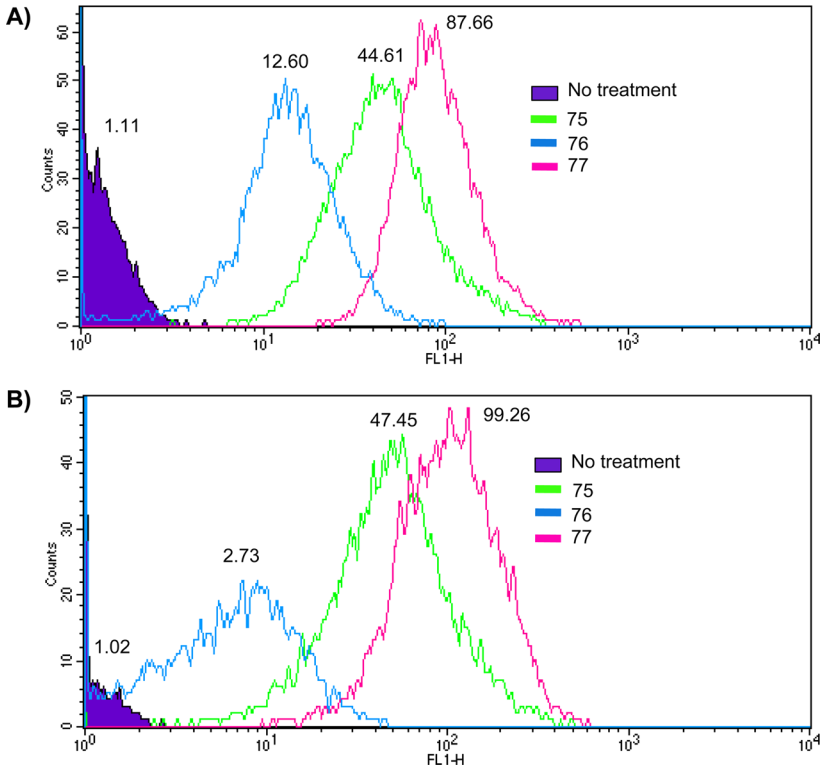

Figure 5. Cellular uptake of the fluorescent ML analogues by DU145 cells. The fluorescent analogue modified with Arg (**76**) showed poor cellular uptake, whereas a compound with an Ile residue (**77**) displayed improved penetration properties when compared to the initial sequence (**75**) containing a Leu residue.

Table 2. Inhibitory Activity and the Selectivity Index Towards PACE4 of the Selected Analogues with Single or Multiple Ile Substitutions[a]

analogue	sequence	K_i PACE4 (nM)	K_i furin (nM)	selectivity index
2	Ac-LLLLRVK[Amba][b]	3.1 ± 0.8	4.3 ± 0.8	1.4
9	Ac-LLLIRVK[Amba]	8 ± 3	27 ± 9	3.4
27	Ac-LLILRVK[Amba]	10 ± 5	30 ± 10	3.0
78	Ac-LLIIRVK[Amba]	9.8 ± 4	8.1 ± 0.5	0.8
79	Ac-[Dleu]LIIRVK[Amba]	14 ± 6	11.7 ± 3.6	0.8
80	Ac-[Dleu]LLLRVK[Amba][c]	4.9 ± 0.9	9.8 ± 2	2.0

[a]The data in the table are the mean values ± SD of three independent experiments. [b]This compound was previously published in ref 20. [c]This compound was previously published in refs 27 and 28.

exhibited improved cell permeability when compared to the initial peptide scaffold (GMFI = 87.66 vs 46.61 without trypsin wash, and GMFI = 99.26 vs 47.45 with trypsin wash). These data demonstrate a significant correlation between the cellular uptake and the antiproliferative activity, indicating that the hydrophobic region (P8−P5) is important for the cell permeability and its disruption with the positively charged amino acid led to an inactive analogue **15**.

Combined Modifications. To investigate whether the selectivity profile of our inhibitors might be improved by the combination of substitutions we design the analogue containing two residues showing the best selectivity profile (analogue **78**). As shown in Table 2, this new inhibitor turned out to be slightly more potent for furin and completely unselective (K_i, 9.8 ± 4 nM for PACE4; K_i, 8.1 ± 0.5 nM for furin). Although both substitutions individually provided an increase in selectivity toward PACE4 (selectivity index for peptide **9**, 3.4, and for peptide **27**, 3.0), the combination of two Ile residues in the position P5 and P6 did not yield a selective inhibitor (selectivity index for peptide **78**, 0.8). However, it should be noted that peptide **78** substituted with combined modification possesses potent antiproliferative effects on both DU145 and LNCaP with IC_{50} of 20 ± 2 and 30 ± 10 μM, respectively (Table 3).

In addition, we prepared the $DLeu^{P8}$-substituted analogue of this peptide (Ac-[DLeu]LIIRVK-Amba, analogue **79**), as it was demonstrated that the incorporation of the DLeu into the structure of peptide **2** resulted in an analogue Ac-[DLeu]-LLLRVK-Amba, known as compound C23 with 2-fold selectivity toward PACE4.[27] However, also in this case we did not observe any improvement in the selectivity profile, and the resulting analogue possessed comparable inhibitory potency against PACE4 and furin (K_i, 14 ± 6 nM for PACE4; K_i, 12 ± 4 nM for furin; Table 2). However, peptide **79**, similar to its counterpart without the DLeu residue, exhibited potent antiproliferative activity on both DU145 and LNCaP with IC_{50} of 37 ± 5 and 60 ± 30 μM, respectively (Table 3).

DOI: 10.1021/acs.jmedchem.6b01499
J. Med. Chem. 2017, 60, 2732−2744

Table 3. Antiproliferative Activity of the Analogues Modified with the Ile Residue in the Comparison with the Initial Scaffolds[a]

analogue	sequence	DU145 IC_{50} (μM) ± SEM	LNCaP IC_{50} (μM) ± SEM
2	Ac-LLLLRVK[Amba][b]	25 ± 10	40 ± 15
9	Ac-LLLIRVK[Amba]	50 ± 10	28 ± 6
27	Ac-LLILRVK[Amba]	32 ± 4	80 ± 10
78	Ac-LLIIRVK[Amba]	20 ± 2	30 ± 10
79	Ac-[DLeu]LIIRVK[Amba]	37 ± 5	60 ± 30
80	Ac-[DLeu]LLLRVK[Amba][c]	25 ± 10	40 ± 10

[a]The concentration of peptides that inhibited cell growth by 50% (IC_{50}) was determined by MTT cell survival assays on DU145 and LNCaP cell lines. The data in the table are the means ± SEM of four independent experiments. [b]This compound was previously published in ref 20. [c]This compound was previously published in refs 27 and 28.

DISCUSSION AND CONCLUSION

The development of PC inhibitors has been the focus of several studies since these enzymes are implicated in various pathologies (review in Couture et al.[2]). PACE4 is involved in prostate cancer progression, and its inhibitors have demonstrated antiproliferative effects on prostate cancer cell lines.[15−17,20] However, the important role of PCs in homeostasis suggests the relevance of developing selective inhibitors with limited inhibitory properties toward other PCs. Our previous study demonstrated that inhibitory selectivity toward PACE4 was achievable with short peptides, as compound **1** that displayed a 20-fold binding affinity for PACE4 over furin (K_i PACE4, 22 ± 6 nM; K_i furin, 430 ± 10 nM).[15] The addition of the Amba moiety into its structure (peptide **2**) resulted in a significant increase in inhibitory potency (K_i PACE4, 3.1 ± 0.8 nM) and an important loss of selectivity (K_i furin, 4.3 ± 0.8 nM).[20] Despite the loss in selectivity, peptide **2** appears as a promising lead compound for drug design because we observed important improvements in stability along with an increase in antiproliferative properties.[20] Of important note, its derivative compound C23 (analogue **80**) was previously shown to inhibit tumor progression in a xenograft model of prostate cancer.[28] A thorough examination of this analogue biodistribution showed adequate tumor delivery and extended *in vivo* stability.[28]

To optimize the selectivity of this drug-candidate, we designed a positional scanning library on the scaffold of peptide **2** to study the molecular determinants within this high affinity PACE4 inhibitor. The library included the canonical recognition pattern described for PCs, modified by the arginine mimetic Amba moiety and an *N*-terminal tetra-Leu sequence (Figure 1). Dahms et al. determined the crystal structure of furin bound to a short, nonspecific Phac-RVR-4-Amba peptide and demonstrated that the rigid Amba moiety was deeply inserted into catalytic pocket, which resulted in tight enclosure of this arginine-mimetic within the S1 subsite.[14] The conformational advantage of the Amba residue led to tight-binding inhibitors, as previously described from enzyme kinetics assays.[20−23,29] In this study, all inhibitors tested presented a high affinity, with K_is in the nanomolar or the picomolar range, consistent with these observations. However, library screening demonstrated that, although the Amba residue encounters a tight binding interaction between the PCs and peptide inhibitors, molecular determinants exist for positions P5 and beyond because differences in binding affinities were observed.

For every position screened, the general trend indicated a preference for basic residues Arg, Lys, and His for both PACE4 and furin (Figure 2). Thus, this observation is in accord with previous positional screening toward furin, which demonstrated that positively charged amino acids were preferred for this enzyme.[30−32] Furthermore, substrate cleavage efficiency studies have previously shown that basic residues in positions P5 and P6 could increase cleavage efficiency by PCs.[33,34] Structural analyses revealed that the PC catalytic cleft is fairly negatively charged, which explains the clear preference for basic residues, as well as the unfavorable presence of the negatively charged amino acid residues Asp and Glu.[11−14] With the exception of charged amino acids, a distinction in binding preferences for large nonpolar aromatic residues was observed for positions P6 and beyond. Indeed, the large amino acid Trp was among the less potent substitution for positions P6 to P8, and Phe offered a slight disadvantage at positions P7 and P8 for both PACE4 and furin. Finally, discrimination in binding preferences could be observed on the basis of hydrophobicity. Whereas the very hydrophobic residue Ile offered a disadvantage toward furin when introduced in positions P5 and P6, this residue was well tolerated in the PACE4 binding cleft. For analogues containing amino acids with shorter aliphatic side chains, Ala and Val, they displayed comparable binding affinities for both enzymes. This result demonstrated that there are differences in subsites S6 and S5 between PACE4 and furin.

It should be mentioned that a previous screen performed on a partial combinatorial library revealed that Leu at the P6 position provides the most selective inhibition toward PACE4 over furin,[15] whereas in the present study its Cβ-branched isomer, Ile, showed the highest selectivity. Unfortunately, with the positional scanning performed in the present study, no peptide containing the Amba moiety displayed a 20-fold selectivity as previously observed for peptide **1**.[15] This can be explained by the tight binding properties of Amba, which stabilizes the active peptide−enzyme complex even with presence of unfavorable residues in positions P5 to P8. Indeed, despite the introduction of negatively charged residues, K_i values remained in the nanomolar range for every position tested. Although they lie outside the canonical recognition pattern for PCs, positions P5 to P7 appear to contribute to the peptides' ability to bind to the furin and PACE4 binding clefts. This study also suggests the limited participation of the position P8 to overall affinity of the peptide **2**. However, this position could be exploited to introduce *N*-terminal peptidomimetic modifications for further optimization of PACE4 inhibitors that could enhance metabolic stability. Indeed, we previously observed that the introduction of the unnatural amino acid, DLeu, in the position P8 of peptide **1** did not alter its affinity toward PACE4, while this substitution in positions P5, P6, and P7 was not tolerated.[20] These results indicate that the P8 residue may be outside the catalytic cleft, thus explaining the tolerance for substitution in this position.

To evaluate the contribution of each substitution on the antiproliferative properties of the peptide **2**, peptides from the P5−P8 libraries were assayed in a proliferation assay using DU145 cells. Only a few peptides in the P5 to P7 libraries demonstrated antiproliferative properties, whereas ten peptides from the P8 library were selected for further analyses on DU145 and LNCaP cells. The scan of the P5 to P8 library in the cell-based assay revealed that the *in vitro* affinity toward PACE4 is not directly informative of a peptide's antiproliferative effects. Indeed, the most potent PACE4 inhibitor tested in

DOI: 10.1021/acs.jmedchem.6b01499
J. Med. Chem. 2017, 60, 2732−2744

the enzyme kinetics assay contained an Arg residue (analogue **15**, K_i PACE4, 0.2 ± 0.1 nM) displayed no antiproliferative effects on DU145 cells (Figure 4). Of note, our previous work has investigated the possibility of cytotoxicity coming from the peptide **2** and its analogues using a membrane integrity assay, which measures the release of lactate dehydrogenase in the media following cell lysis. These studies have shown that compound **2** (at the 100 μM concentration) after 4 h incubation with DU145 cell led to less than 5% cell death, suggesting that the calculated IC_{50}s values are the result of antiproliferative properties rather than cytotoxic effects from this series of peptide.[20] Using the FITC-labeled version of analogue **15**, we demonstrate that it has significantly reduced cellular uptake when compared to analogues with hydrophobic Leu or Ile residue at this position (Figure 5). These data strongly support our previous observations that inhibitor **1** or its analogues have to target intracellular PACE4 to induce an antiproliferative response.[15] The incorporation of the charged side chain into the tetra-leucine core diminished its cell penetration properties, possibly caused by disruption of the amphipathic structure of inhibitor **2**.

Amphipathic peptides are known to enter cells by an endocytosis-independent mechanism, likely through direct interactions with the membrane bilayer and membrane disorganization, which leads to a broad cellular distribution of those peptides.[35−37] Inhibitor **1** and its analogues display excellent cell penetration properties, and analyses of cellular localization indicated a broad cellular presence of its FITC-labeled analogue when incubated with cells.[15] In this study, only peptides containing hydrophobic residues, with the exception of an analogue having Gln at the P5 position, displayed potent antiproliferative effects on DU145 and LNCaP cells. Therefore, preservation of the amphiphilic character should be considered upon designing new PACE4 inhibitors.

Despite the beneficial effect on the selectivity profile of Ile-substituted peptides (analogue **9** and **27**, 3-fold improvement), their combination enhanced binding affinity for furin and resulted in an unselective analogue **78** (Table 2), indicating that binding sites of furin exhibit some degree of cooperativity. This phenomenon has been already observed in a wide range of proteases,[38] including the proprotein convertase yeast homologue kexin, where binding of a particular amino acid was shown to be influenced by the neighboring residue within positions P1 to P4.[39] These results demonstrated that in the case of our starting inhibitor **2** only the single substitution Ile at the P5 or P6 position is well tolerated and provides some degree of discrimination between furin and PACE4. This indicates that an alternative approach such as targeting allosteric sites and exosites (alone or together with the active sites) should be considered to optimize the selectivity profile of PACE4 inhibitors. This strategy has been proven successful to generate new anticoagulants, i.e., highly selective thrombin inhibitors known as bivalent direct thrombin inhibitors (hirudin-derived peptides),[40] which bind simultaneously to the catalytic site and exosite 1 domain of thrombin.[41] The importance of "adventitious binding points" has been also investigated for protein-based PCs inhibitors. It has been shown that engineered variants of eglin c exhibited enhanced selectivity toward target enzyme (e.g., up 41-fold for furin versus PC7 and 20-fold for PC7 versus furin).[42] However, until now, to the best of our knowledge, no exosites or allosteric sites have been identified for PCs.

In regards to the eventual use of PACE4 inhibitors as antiproliferative agents in prostate cancer, it has not yet been determined if these compounds have secondary effects. In a recent study, it was shown that PACE4 is an enzyme responsible for the activation of Corin, also an enzyme that generates the natriuretic peptides in the heart.[43] It was thus speculated that PACE4 inhibition might result in cardiovascular side effects. However, in our hands, the presently described PACE4 inhibitors do not produce any hypertensive effects. Furthermore, PACE4 knockout mice are not hypertensive under normal conditions (unpublished data).

In conclusion, this article demonstrates that molecular determinants for PACE4 and furin exist within subsites S5 to S7. However, the influence of amino acid substitution appeared attenuated with the presence of the Amba moiety in the P1 position, leading to high affinity inhibitors of both PCs even in the presence of unfavorable residues in positions P5 and beyond. Only the incorporation of the Ile residue offered a 3-fold inhibitory selectivity toward PACE4 when introduced within position P5 or P6 of the starting peptide. Furthermore, the presence of this highly hydrophobic amino acid residue at these positions sustained the amphipathic nature of peptide **2** and the antiproliferative effects observed toward prostate cancer cell lines. The findings described here could be used to guide the design of a new generation of PACE4 inhibitors with improved selectivity and activity for potential therapeutic applications. As regard to therapeutic applications of PACE4 inhibitors, a potent and stable yet less selective analogue might be suitable. Further optimization of therapeutic regimens or targeted delivery could offer practical therapeutic index.

EXPERIMENTAL SECTION

Peptide Synthesis. Fmoc amino acids, resins, coupling reagents, and solvents were purchased from GL Biochem, Merck Chemicals, Rapp Polymere, and Sigma-Aldrich. Fmoc-SPPS (Fmoc/*t*Bu strategy) was performed manually or on an automatic synthesizer Symphony (Protein Technologies, USA). Protected 4-amidinobenzylamine and 4-amidinobenzylamine·2HCl were synthesized using protocols described in the literature.[20,23,44−46]

All P5-substituted peptides were synthesized on a 4-Fmoc-hydrazinobenzoyl AM NovaGel resin (substitution 0.49 mmol/g), with the exception of the analogue modified with the Met residue. After removing the protecting group from the resin using a standard procedure, the Ac-P8-P2 fragment of the peptide was synthesized using a Symphony (Protein Technologies, USA) automatic synthesizer as described in Scheme 1. During the synthesis, amino acid coupling was performed using 2.5 equiv of amino acid, 2.5 equiv of *O*-(benzotriazol-1-yl)-*N*,*N*,*N*′,*N*′-tetramethyluronium tetrafluoroborate (TBTU), 2.5 equiv of 1-hydroxybenzotriazole (HOBt) as coupling reagents, and 5 equiv of *N*-methylmorpholine (NMM). N-Terminal acetylation was performed three times with acetic anhydride/diisopropylethylamine (DIPEA)/dichloromethane (DCM) (1.5/1.5/7, v/v/v) for 10 min. Peptidyl resin oxidation and coupling of the protected 4-amidinobenzylamine were performed manually with 2.5 equiv of the compound, 0.7 equiv of $Cu(OAc)_2$, and 1.5 equiv of pyridine in anhydrous *N*,*N*-dimethylformamide (DMF) for 24 h.[47−49] The resin was drained, and DMF was removed *in vacuo*. The protecting groups were removed from side chains using a standard mixture of trifluoroacetic acid (TFA)/triisopropylsilane (TIS)/H_2O (95/2.5/2.5, v/v/v) for 2.5 h. The solvents were removed *in vacuo*, and the inhibitors were precipitated with ether, centrifuged, and lyophilized from 30% acetonitrile in water. The peptides were then dissolved in acetic acid/methanol (MeOH) (1/1, v/v), diluted to a 1 M concentration, treated with catalyst (10% Pd/C), and hydrogenated using a shaker-type hydrogenation apparatus 3911 (Paar, USA) (1.5 h, 55 psi, RT). The catalyst was filtered and washed with MeOH, and

DOI: 10.1021/acs.jmedchem.6b01499
J. Med. Chem. 2017, 60, 2732−2744

solvents were removed *in vacuo*. The product was diluted in 20% acetonitrile in water, lyophilized, and purified by preparative HPLC (system Waters; purity > 98%).

Compound **11**, all peptides substituted at the P6, P7, and P8 positions, inhibitors with multiple substitutions, and FITC-modified analogues were prepared using a combination of SPPS and solution-phase synthesis as shown in Scheme 2. The loading of the first amino acid on the 2-chlorotrityl-chloride resin was prepared using 2 equiv of Fmoc-Lys(Boc)-OH, dissolved in dry DCM (10 mL per 1 g of resin), and rapid addition of 2 equiv of DIPEA to the resin. After 1 h, MeOH was added (2−4 mL per 1 g of resin), and the mixture was stirred for 15 min. The resin was drained and washed with DCM, DMF, and DCM and dried *in vacuo*. Fmoc SPPS was continued manually or with an automatic synthesizer using the same procedure as for the peptides presented above. For the FITC-labeled peptides, in the last step the resin was treated with a solution of 3 equiv of FITC in pyridine/DCM (1:4 v/v) and agitated on the automated shaker for 16 h in room temperature. The resin was filtrated and washed successively with acetonitrile (ACN), DMF, isopropanol, and DCM. Then, peptidyl resins were treated as their counterparts without the FITC moiety. Cleavage of fully protected peptides was obtained by treatment with hexafluoroisopropanol (HFIP)/trifluoroethanol (TFE)/dichloromethane (DCM) (3/2/5, v/v/v) for 2 h at RT. After solvent removal *in vacuo*, the analogues were precipitated with cold diethyl ether, centrifuged, and lyophilized from 50% *tert*-butanol in water. Coupling of the protected 4-amidinobenzylamine or 4-amidinobenzylamine·2HCl was carried in solution using 2 equiv of this compound, 2 equiv of (1-cyano-2-ethoxy-2-oxoethylidenaminooxy)-dimethylaminomorpholino-carbenium hexafluorophosphate (COMU), and 8 equiv of NMM or 6 equiv of DIPEA in anhydrous DMF overnight as described previously.[20] DMF was removed, and side group deprotection and hydrogenation were performed as described above. The peptide was diluted in 20% ACN in water, lyophilized, and purified by reversed phase preparative HPLC to achieve a purity of >98% using a Waters system (Kromasil 100 C8 column, 250 × 16 mm, 5 μm) with a linear gradient of 80% ACN in water containing 0.1% of TFA from 13 to 43%, 13 to 50%, or 20 to 65% for 90 min at a flow rate of 8 mL/min, a Shimadzu system (Jupiter 4 μ Proteo column, 90 Å, 250 × 10 mm) with a linear gradient of ACN from 20 to 60% for 50 min at a flow rate of 4 mL/min, or a VARIAN ProStar system (Phenomenex Jupiter C18 column, 300 Å, 250 × 21.20 mm, 5 μm) with a linear gradient of ACN from 25 to 50% for 55 min a flow rate of 7 mL/min. All inhibitors were finally obtained as TFA salts after lyophilization.

Inhibitor purity was determined using an Agilent analytical RP-HPLC system (VYDAC C_{18} or AGILENT Elipse XDB C_{18} column) and a Shimadzu RP-HPLC system (Jupiter 4 μ Proteo 90 Å, 250 × 4.60 mm). The molecular masses of the synthesized compounds were verified using LCMS ESI IT-TOF (Shimadzu, Japan) or HRMS (TripleTOF 5600, ABSciex, USA) mass spectrometers. The physicochemical properties of all analogues are presented as Supporting Information in Table S1. All tested compounds possess purity of at least 98% (for FITC-peptides at least 95%).

Enzymatic Assays. The inhibition constants (K_i) were determined using human recombinant PCs (PACE4 and furin) that were produced and purified as described previously.[50] Competitive assays were performed in 96-well microtiter plates for 60 min at 37 °C with 100 μM of the fluorogenic substrate *pyr*Glu-Arg-Thr-Lys-Arg-7-amido-4-methylcoumarin (Bachem, CA, USA) and different inhibitor concentrations (ranging from 10 μM to 1 nM). The enzymes were added at a final concentration of 2 units per 100 μL in each well (PACE4, 20.18 nM; furin, 0.54 nM), and fluorescence was measured using a Gemini XS spectrofluorometer equipped with SoftMaxPro5 (Molecular Devices, CA) (λ_{EX}, 370 nm; λ_{EM}, 460 nm; cutoff, 435 nm). K_i values were calculated from the Morrison equation for tight binding inhibitors using Prism 5.0 (GraphPad Software, CA, USA) as described previously.[20] The Michaelis−Menten constants (K_M) for PACE4 and furin are 4.035 and 5.04 μM, respectively. K_is were determined in three independent experiments for each peptide, and the results presented in Figure 4 and Table 1 are the mean ± standard deviation.

Assays with PACE4 were carried out in 20 mM BisTris pH 6.5, 1 mM $CaCl_2$, and 1.8 mg/mL BSA buffer. Furin enzymatic assays were carried out in 100 mM HEPES, pH 7.5, 1 mM $CaCl_2$, 1 mM β-mercaptoethanol, and 1.8 mg/mL BSA, except for His containing peptides, which were performed in 20 mM BisTris pH 6.5, 1 mM $CaCl_2$, 1 mM β-mercaptoethanol, and 1.8 mg/mL BSA. The inhibition assays of peptides containing His residues were performed at pH 6.5 to ensure similar ionization of this residue and to allow for proper comparison of the binding properties between PACE4 and furin, given that the His side chain pK_a is 6.08.

Proliferation Assays. Prostate cancer cell lines were obtained from ATCC and maintained at 37 °C in a water-saturated atmosphere with 5% CO_2 in RPMI 1640 medium supplemented with either 5% fetal bovine serum (FBS; Wisent Bioproducts, Canada) for DU145 or 10% FBS for LNCaP. The MTT proliferation assay was performed as described previously.[15,20] Briefly, DU145 cells were seeded at a density of 1500 cells/well, and LNCaP cells were seeded at a density of 2500 cells/well in a poly-L-lysine coated plate. Twenty-four hours after cell plating, the inhibitors were added to the cells in fresh FBS-supplemented media. A first screen of the antiproliferative properties was performed using inhibitor doses of 25, 50, and 100 μM (Figure 4) with DU145 cells, and complete dose−response curves were then determined with inhibitor doses of 0, 1, 10, 25, 50, 75, 100, and 250 μM on DU145 and LNCaP cells (Table 1). The peptide inhibitors were incubated with the cells for 72 h, and metabolic activity was evaluated by adding the MTT reagent to the DU145 and LNCaP cells at final concentration of 1 mg/mL for 4 h. The formazan salt was solubilized with 100 μL of 2-propanol HCl (24:1 N), and the total metabolic activity was normalized relatively to vehicle-treated cells (sterile bidistilled water). The half-maximal inhibitory concentration (IC_{50}) was calculated using Prism 5.0 (GraphPad Software, USA). The proliferation assay results are the mean ± standard deviation from at least three independent experiments (n = 3).

Cell Penetration. The cell penetration assays were performed on DU145 cells using FITC-labeled peptides. Briefly, DU145 cells were incubated for 1 h in serum-free RPMI media with 10 μM of the FITC-analogue and collected by trypsin−EDTA digestion followed by centrifugation. Cells in suspension were then extensively washed twice with trypsin (0.05% v/v) for 5 min at 37 °C to remove nonspecific interactions with the membrane proteins. Then, cells were incubated for 2 min with propidium iodine (10 μg/mL) to exclude cells with altered membrane and were immediately analyzed (10000 events/sample) by fluorescence activated cell sorting (FACS; Becton Dickinson; Mountain View, CA, USA). GeoMeans were determined using CellQuest Software (Becton Dickinson).

■ ASSOCIATED CONTENT

Supporting Information

The Supporting Information is available free of charge on the ACS Publications website at DOI: 10.1021/acs.jmedchem.6b01499.

Analytical data (HPLC and MS) for all the analogues (PDF)

■ AUTHOR INFORMATION

Corresponding Authors

*(A.K.) Telephone: 819-821-8000, ext. 70110. E-mail: anna.kwiatkowska@usherbrooke.ca.

*(R.D.) Telephone: 819 821-8000, ext. 75428. E-mail: robert.day@usherbrooke.ca.

ORCID

Anna Kwiatkowska: 0000-0002-5659-3680

Author Contributions

#I.M. and C.L. contributed equally to this work.

DOI: 10.1021/acs.jmedchem.6b01499
J. Med. Chem. 2017, 60, 2732−2744

Notes

The authors declare no competing financial interest.

■ ACKNOWLEDGMENTS

This research was financed by the Canadian Cancer Society Research Institute (Impact grant # 701590), Prostate Cancer Canada and the Movember Foundation (grants #2012-951 and #D2013-8 and TAG2014-02), and the Fondation Mon Étoile (http://fondationmonetoile.org) to R.D. This research was also supported in part by the National Science Centre Poland (DEC-2012/05/N/ST5/01080) to I.M. F.C. holds a Banting and Charles Best Canada Graduate Scholarships (grant #315690) from CIHR and Graduate Studentship from Prostate Cancer Canada (Grant #GS-2015-07). The authors thank Xue Wen Yuan for assistance with peptide synthesis. We also thank Dr. Leonid Volkov for his help with flow cytometry, and Dr. Hugo Gagnon (PhenoSwitch Biosciences Inc.) for high-resolution mass spectrometry analysis.

■ ABBREVIATIONS

ACN, acetonitrile; Amba, 4-amidinobenzylamide; COMU, 1-cyano-2-ethoxy-2-oxoethylidenaminooxy)-dimethylaminomorpholino-carbenium-hexafluoro phosphate; DCM, dichloromethane; DIPEA, diisopropylethylamine; DMF, *N*,*N*-dimethylformamide; DMSO, dimethyl sulfoxide; FACS, fluorescence-activated cell sorting; FBS, Fetal Bovine Serum; FITC, fluorescein isothiocyanate; GMFI, geometric mean of fluorescence intensity; HFIP, hexafluoroisopropanol; HOBt, 1-hydroxybenzotriazole; HRMS, high-resolution mass spectrometry; IC_{50}, half-maximal inhibitory concentration; K_i, inhibition constant; LCMS ESI IT-TOF, liquid chromatography−mass spectrometry system with electrospray ionization connective ion trap and time-of-flight analyzers; ML, multi-Leu peptide inhibitor; NMM, *N*-methylmorpholine; PC, proprotein convertase; RP-HPLC, reversed-phase high-performance liquid chromatography; SPPS, solid-phase peptide synthesis; TBTU, *O*-(benzotriazol-1-yl)-*N*,*N*,*N*′,*N*′-tetramethyluronium tetrafluoroborate; TFA, trifluoroacetic acid; TFE, trifluoroethanol; TIS, triisopropylsilane

■ REFERENCES

(1) Seidah, N. G.; Prat, A. The biology and therapeutic targeting of the proprotein convertases. *Nat. Rev. Drug Discovery* **2012**, *11*, 367−383.
(2) Couture, F.; D'Anjou, F.; Day, R. On the cutting edge of proprotein convertase pharmacology: from molecular concepts to clinical applications. *Biomol. Concepts* **2011**, *2*, 421−438.
(3) Fugère, M.; Day, R. Cutting back on pro-protein convertases: the latest approaches to pharmacological inhibition. *Trends Pharmacol. Sci.* **2005**, *26*, 294−301.
(4) Taylor, N. A.; Van De Ven, W. J.; Creemers, J. W. Curbing activation: proprotein convertases in homeostasis and pathology. *FASEB J.* **2003**, *17*, 1215−1227.
(5) Thomas, G. Furin at the cutting edge: from protein traffic to embryogenesis and disease. *Nat. Rev. Mol. Cell Biol.* **2002**, *3*, 753−766.
(6) Bergeron, F.; Leduc, R.; Day, R. Subtilase-like pro-protein convertases: from molecular specificity to therapeutic applications. *J. Mol. Endocrinol.* **2000**, *24*, 1−22.
(7) Creemers, J. W.; Khatib, A. M. Knock-out mouse models of proprotein convertases: unique functions or redundancy? *Front. Biosci., Landmark Ed.* **2008**, *13*, 4960−4971.
(8) Seidah, N. G.; Sadr, M. S.; Chretien, M.; Mbikay, M. The multifaceted proprotein convertases: their unique, redundant, complementary, and opposite functions. *J. Biol. Chem.* **2013**, *288*, 21473−21481.
(9) Scamuffa, N.; Calvo, F.; Chretien, M.; Seidah, N. G.; Khatib, A. M. Proprotein convertases: lessons from knockouts. *FASEB J.* **2006**, *20*, 1954−1963.
(10) Artenstein, A. W.; Opal, S. M. Proprotein convertases in health and disease. *N. Engl. J. Med.* **2011**, *365*, 2507−2518.
(11) Henrich, S.; Cameron, A.; Bourenkov, G. P.; Kiefersauer, R.; Huber, R.; Lindberg, I.; Bode, W.; Than, M. E. The crystal structure of the proprotein processing proteinase furin explains its stringent specificity. *Nat. Struct. Biol.* **2003**, *10*, 520−526.
(12) Henrich, S.; Lindberg, I.; Bode, W.; Than, M. E. Proprotein convertase models based on the crystal structures of furin and kexin: explanation of their specificity. *J. Mol. Biol.* **2005**, *345*, 211−227.
(13) Tian, S.; Jianhua, W. Comparative study of the binding pockets of mammalian proprotein convertases and its implications for the design of specific small molecule inhibitors. *Int. J. Biol. Sci.* **2010**, *6*, 89−95.
(14) Dahms, S. O.; Hardes, K.; Becker, G. L.; Steinmetzer, T.; Brandstetter, H.; Than, M. E. X-ray structures of human furin in complex with competitive inhibitors. *ACS Chem. Biol.* **2014**, *9*, 1113−1118.
(15) Levesque, C.; Fugere, M.; Kwiatkowska, A.; Couture, F.; Desjardins, R.; Routhier, S.; Moussette, P.; Prahl, A.; Lammek, B.; Appel, J. R.; Houghten, R. A.; D'Anjou, F.; Dory, Y. L.; Neugebauer, W.; Day, R. The multi-leu peptide inhibitor discriminates between PACE4 and furin and exhibits antiproliferative effects on prostate cancer cells. *J. Med. Chem.* **2012**, *55*, 10501−10511.
(16) D'Anjou, F.; Routhier, S.; Perreault, J. P.; Latil, A.; Bonnel, D.; Fournier, I.; Salzet, M.; Day, R. Molecular validation of PACE4 as a target in prostate cancer. *Transl. Oncol.* **2011**, *4*, 157−172.
(17) Couture, F.; D'Anjou, F.; Desjardins, R.; Boudreau, F.; Day, R. Role of proprotein convertases in prostate cancer progression. *Neoplasia* **2012**, *14*, 1032−1042.
(18) Kang, S.; Zhao, Y.; Hu, K.; Xu, C.; Wang, L.; Liu, J.; Yao, A.; Zhang, H.; Cao, F. miR-124 exhibits antiproliferative and antiaggressive effects on prostate cancer cells through PACE4 pathway. *Prostate* **2014**, *74*, 1095−1106.
(19) Klee, E. W.; Bondar, O. P.; Goodmanson, M. K.; Dyer, R. B.; Erdogan, S.; Bergstralh, E. J.; Bergen, H. R., 3rd; Sebo, T. J.; Klee, G. G. Candidate serum biomarkers for prostate adenocarcinoma identified by mRNA differences in prostate tissue and verified with protein measurements in tissue and blood. *Clin. Chem.* **2012**, *58*, 599−609.
(20) Kwiatkowska, A.; Couture, F.; Levesque, C.; Ly, K.; Desjardins, R.; Beauchemin, S.; Prahl, A.; Lammek, B.; Neugebauer, W.; Dory, Y. L.; Day, R. Design, synthesis, and structure-activity relationship studies of a potent PACE4 inhibitor. *J. Med. Chem.* **2014**, *57*, 98−109.
(21) Becker, G. L.; Hardes, K.; Steinmetzer, T. New substrate analogue furin inhibitors derived from 4-amidinobenzylamide. *Bioorg. Med. Chem. Lett.* **2011**, *21*, 4695−4697.
(22) Becker, G. L.; Lu, Y.; Hardes, K.; Strehlow, B.; Levesque, C.; Lindberg, I.; Sandvig, K.; Bakowsky, U.; Day, R.; Garten, W.; Steinmetzer, T. Highly potent inhibitors of proprotein convertase furin as potential drugs for treatment of infectious diseases. *J. Biol. Chem.* **2012**, *287*, 21992−22003.
(23) Becker, G. L.; Sielaff, F.; Than, M. E.; Lindberg, I.; Routhier, S.; Day, R.; Lu, Y.; Garten, W.; Steinmetzer, T. Potent inhibitors of furin and furin-like proprotein convertases containing decarboxylated P1 arginine mimetics. *J. Med. Chem.* **2010**, *53*, 1067−1075.
(24) Morrison, J. F. Kinetics of the reversible inhibition of enzyme-catalysed reactions by tight-binding inhibitors. *Biochim. Biophys. Acta* **1969**, *185*, 269−286.
(25) Williams, J. W.; Morrison, J. F. The kinetics of reversible tight-binding inhibition. *Methods Enzymol.* **1979**, *63*, 437−467.
(26) Eisenberg, D. Three-dimensional structure of membrane and surface proteins. *Annu. Rev. Biochem.* **1984**, *53*, 595−623.
(27) Kwiatkowska, A.; Couture, F.; Levesque, C.; Ly, K.; Beauchemin, S.; Desjardins, R.; Neugebauer, W.; Dory, Y. L.; Day, R. Novel insights into structure-activity relationships of N-terminally modified PACE4 inhibitors. *ChemMedChem* **2016**, *11*, 289−301.

DOI: 10.1021/acs.jmedchem.6b01499
J. Med. Chem. 2017, 60, 2732−2744

(28) Levesque, C.; Couture, F.; Kwiatkowska, A.; Desjardins, R.; Guerin, B.; Neugebauer, W. A.; Day, R. PACE4 inhibitors and their peptidomimetic analogs block prostate cancer tumor progression through quiescence induction, increased apoptosis and impaired neovascularisation. *Oncotarget* **2015**, *6*, 3680−3693.
(29) Gagnon, H.; Beauchemin, S.; Kwiatkowska, A.; Couture, F.; D'Anjou, F.; Levesque, C.; Dufour, F.; Desbiens, A. R.; Vaillancourt, R.; Bernard, S.; Desjardins, R.; Malouin, F.; Dory, Y. L.; Day, R. Optimization of furin inhibitors to protect against the activation of influenza hemagglutinin H5 and shiga toxin. *J. Med. Chem.* **2014**, *57*, 29−41.
(30) Kacprzak, M. M.; Peinado, J. R.; Than, M. E.; Appel, J.; Henrich, S.; Lipkind, G.; Houghten, R. A.; Bode, W.; Lindberg, I. Inhibition of furin by polyarginine-containing peptides: nanomolar inhibition by nona-D-arginine. *J. Biol. Chem.* **2004**, *279*, 36788−36794.
(31) Cameron, A.; Appel, J.; Houghten, R. A.; Lindberg, I. Polyarginines are potent furin inhibitors. *J. Biol. Chem.* **2000**, *275*, 36741−36749.
(32) Remacle, A. G.; Shiryaev, S. A.; Oh, E. S.; Cieplak, P.; Srinivasan, A.; Wei, G.; Liddington, R. C.; Ratnikov, B. I.; Parent, A.; Desjardins, R.; Day, R.; Smith, J. W.; Lebl, M.; Strongin, A. Y. Substrate cleavage analysis of furin and related proprotein convertases. A comparative study. *J. Biol. Chem.* **2008**, *283*, 20897−20906.
(33) Tian, S. A 20 residues motif delineates the furin cleavage site and its physical properties may influence viral fusion. *Biochem. Insights* **2009**, *2*, 9−20.
(34) Krysan, D. J.; Rockwell, N. C.; Fuller, R. S. Quantitative characterization of furin specificity. Energetics of substrate discrimination using an internally consistent set of hexapeptidyl methylcoumarinamides. *J. Biol. Chem.* **1999**, *274*, 23229−23234.
(35) Heitz, F.; Morris, M. C.; Divita, G. Twenty years of cell-penetrating peptides: from molecular mechanisms to therapeutics. *Br. J. Pharmacol.* **2009**, *157*, 195−206.
(36) Deshayes, S.; Plenat, T.; Aldrian-Herrada, G.; Divita, G.; Le Grimellec, C.; Heitz, F. Primary amphipathic cell-penetrating peptides: structural requirements and interactions with model membranes. *Biochemistry* **2004**, *43*, 7698−7706.
(37) Deshayes, S.; Plenat, T.; Charnet, P.; Divita, G.; Molle, G.; Heitz, F. Formation of transmembrane ionic channels of primary amphipathic cell-penetrating peptides. Consequences on the mechanism of cell penetration. *Biochim. Biophys. Acta, Biomembr.* **2006**, *1758*, 1846−1851.
(38) Ng, N. M.; Pike, R. N.; Boyd, S. E. Subsite cooperativity in protease specificity. *Biol. Chem.* **2009**, *390*, 401−407.
(39) Rockwell, N. C.; Fuller, R. S. Interplay between S1 and S4 subsites in Kex2 protease: Kex2 exhibits dual specificity for the P4 side chain. *Biochemistry* **1998**, *37*, 3386−3391.
(40) Lee, C. J.; Ansell, J. E. Direct thrombin inhibitors. *Br. J. Clin. Pharmacol.* **2011**, *72*, 581−592.
(41) Alban, S. Pharmacological strategies for inhibition of thrombin activity. *Curr. Pharm. Des.* **2008**, *14*, 1152−1175.
(42) Komiyama, T.; VanderLugt, B.; Fugere, M.; Day, R.; Kaufman, R. J.; Fuller, R. S. Optimization of protease-inhibitor interactions by randomizing adventitious contacts. *Proc. Natl. Acad. Sci. U. S. A.* **2003**, *100*, 8205−8210.
(43) Chen, S.; Cao, P.; Dong, N.; Peng, J.; Zhang, C.; Wang, H.; Zhou, T.; Yang, J.; Zhang, Y.; Martelli, E. E.; Naga Prasad, S. V.; Miller, R. E.; Malfait, A. M.; Zhou, Y.; Wu, Q. PCSK6-mediated Corin activation is essential for normal blood pressure. *Nat. Med. (N. Y., NY, U. S.)* **2015**, *21*, 1048−1053.
(44) Judkins, B. D.; Allen, D. G.; Cook, T. A.; Evans, B.; Sardharwala, T. E. A versatile synthesis of amidines from nitriles via amidoximes. *Synth. Commun.* **1996**, *26*, 4351−4367.
(45) Bakunova, S. M.; Bakunov, S. A.; Wenzler, T.; Barszcz, T.; Werbovetz, K. A.; Brun, R.; Tidwell, R. R. Synthesis and antiprotozoal activity of pyridyl analogues of pentamidine. *J. Med. Chem.* **2009**, *52*, 4657−4667.
(46) Kunzel, S.; Schweinitz, A.; Reissmann, S.; Sturzebecher, J.; Steinmetzer, T. 4-amidinobenzylamine-based inhibitors of urokinase. *Bioorg. Med. Chem. Lett.* **2002**, *12*, 645−648.
(47) Millington, C. R.; Quarrell, R.; Lowe, G. Aryl hydrazides as linkers for solid phase synthesis which are cleavable under mild oxidative conditions. *Tetrahedron Lett.* **1998**, *39*, 7201−7204.
(48) Kwon, Y.; Welsh, K.; Mitchell, A. R.; Camarero, J. A. Preparation of peptide p-nitroanilides using an aryl hydrazine resin. *Org. Lett.* **2004**, *6*, 3801−3804.
(49) Woo, Y.-H.; Mitchell, A.; Camarero, J. The use of aryl hydrazide linkers for the solid phase synthesis of chemically modified peptides. *Int. J. Pept. Res. Ther.* **2007**, *13*, 181−190.
(50) Fugère, M.; Limperis, P. C.; Beaulieu-Audy, V.; Gagnon, F.; Lavigne, P.; Klarskov, K.; Leduc, R.; Day, R. Inhibitory potency and specificity of subtilase-like pro-protein convertase (SPC) prodomains. *J. Biol. Chem.* **2002**, *277*, 7648−7656.

DOI: 10.1021/acs.jmedchem.6b01499
J. Med. Chem. 2017, 60, 2732−2744